Cancer Cell
Article

The Glycolytic Shift in Fumarate-Hydratase-Deficient Kidney Cancer Lowers AMPK Levels, Increases Anabolic Propensities and Lowers Cellular Iron Levels

Wing-Hang Tong,[1] Carole Sourbier,[2] Gennady Kovtunovych,[1] Suh Young Jeong,[1] Manish Vira,[3] Manik Ghosh,[1] Vladimir Valera Romero,[2] Rachid Sougrat,[4] Sophie Vaulont,[5,6] Benoit Viollet,[5,6] Yeong-Sang Kim,[7] Sunmin Lee,[7] Jane Trepel,[7] Ramaprasad Srinivasan,[2] Gennady Bratslavsky,[2] Youfeng Yang,[2] W. Marston Linehan,[2,*] and Tracey A. Rouault[1,*]

[1]Molecular Medicine Program, Eunice Kennedy Shriver National Institute of Child Health and Development, Bethesda, Maryland, USA
[2]Urologic Oncology Branch, Center for Cancer Research, National Cancer Institute, Bethesda, Maryland, USA
[3]Albert Einstein College of Medicine, New York, USA
[4]King Abdullah University of Science and Technology, Saudi Arabia
[5]Institut Cochin, Université Paris Descartes, CNRS (UMR8104), Paris, France
[6]Inserm U 1016, Paris, France
[7]Medical Oncology Branch, National Cancer Institute, Bethesda, Maryland, USA
*Correspondence: rouault@mail.nih.gov (T.A.R.), WML@nih.gov (W.M.L.)
DOI 10.1016/j.ccr.2011.07.018

SUMMARY

Inactivation of the TCA cycle enzyme, fumarate hydratase (*FH*), drives a metabolic shift to aerobic glycolysis in *FH*-deficient kidney tumors and cell lines from patients with hereditary leiomyomatosis renal cell cancer (HLRCC), resulting in decreased levels of AMP-activated kinase (AMPK) and p53 tumor suppressor, and activation of the anabolic factors, acetyl-CoA carboxylase and ribosomal protein S6. Reduced AMPK levels lead to diminished expression of the DMT1 iron transporter, and the resulting cytosolic iron deficiency activates the iron regulatory proteins, IRP1 and IRP2, and increases expression of the hypoxia inducible factor HIF-1α, but not HIF-2α. Silencing of HIF-1α or activation of AMPK diminishes invasive activities, indicating that alterations of HIF-1α and AMPK contribute to the oncogenic growth of FH-deficient cells.

INTRODUCTION

Understanding the underlying mechanisms of metabolic alterations in cancer, particularly the metabolic shift to aerobic glycolysis, has the potential to improve cancer diagnosis and provide the foundation for novel therapeutic approaches (Kaelin and Thompson, 2010). The TCA cycle plays a key role in energy production as well as biosynthesis of lipid and amino acids, and mutations of the TCA cycle genes, fumarate hydratase (*FH*) and succinate dehydrogenase (SDH), are associated with tumor formation (Baysal et al., 2000; King et al., 2006; Tomlinson et al., 2002; Toro et al., 2003). Germline mutations of *FH* are associated with the development of hereditary leiomyomatosis and renal cell cancer (HLRCC) (Tomlinson et al., 2002), whereas germline mutations in SDH are associated with paragangliomas (PGL), pheochromocytomas (PHEO), and renal cell carcinoma (RCC) (Baysal et al., 2000; Hao et al., 2009). HLRCC patients are predisposed to the development of cutaneous and uterine leiomyomas and an aggressive form of type II papillary kidney cancer that is characterized by distinctive architectural and morphologic features (Launonen et al., 2001; Merino et al., 2007). HLRCC renal tumors differ from other genetically defined types of hereditary renal cancers in that they often present as solitary lesions with a propensity to metastasize early to regional

Significance

A hallmark of tumor cells is the metabolic shift from oxidative phosphorylation to aerobic glycolysis (the Warburg effect). Herein, we demonstrate that inactivation of the TCA cycle drives a glycolytic shift and decreases the levels of the master metabolic regulator, AMPK. Increased glycolysis confers growth advantages by diverting glucose to generate NADPH, acetyl-CoA, and ribose; reduced AMPK signaling suppresses p53 expression and activates factors involved in protein and fatty acid biosynthesis. Furthermore, reduced AMPK signaling decreases the expression of the DMT1 iron transporter, which contributes to elevation of HIF-1α, a key activator of glycolysis. Together, the changes in AMPK, p53, and HIF define a unique metabolic profile that distinguishes fumarate hydratase-deficient cancer from other genetically defined renal cell carcinomas.

and distant lymph nodes. Previous studies have shown that *FH* deficiency results in the accumulation of fumarate, which inhibits prolyl hydroxylases (PHDs) and impairs HIF-1α and HIF-2α degradation (Isaacs et al., 2005; Pollard et al., 2005). Accumulation of HIF has been proposed to promote tumorigenesis through dysregulation of growth factors VEGF, TGF-α and PDGF, the Glut-1 glucose transporter, and glycolytic enzymes (Isaacs et al., 2005; Pollard et al., 2005; 2007; Semenza, 2009).

Recently, UOK262, a kidney cancer cell line derived from a retroperitoneal metastasis in a patient with recurrent HLRCC kidney cancer (Yang et al., 2010), exhibited "precisely the properties expected of a Warburg tumor" (Bayley and Devilee, 2010). Warburg observed that cancer cells depend on glycolysis rather than oxidative phosphorylation (OXPHOS) for energy production and he theorized that abnormalities in mitochondrial energy production constituted a central aspect of carcinogenesis (DeBerardinis et al., 2008; Warburg, 1956). In UOK262 cells, loss of functional *FH* impairs the TCA cycle, imposing a need for metabolic transformation. As a result, UOK262 cells exhibit extremely low respiration rates, elevated levels of HIF-1α and Glut-1, increased glucose dependence, and increased lactate production (Sudarshan et al., 2009; Yang et al., 2010).

The AMP-activated protein kinase (AMPK) plays a key role in intracellular metabolic sensing and adaptation (Hardie, 2007) and occupies a central position in a complex metabolic network implicated in tumor formation (Jones and Thompson, 2009; Luo et al., 2005). AMPK is a highly conserved heterotrimeric serine/threonine protein kinase complex composed of a catalytic α subunit and regulatory β and γ subunits, each of which is encoded by two or three distinct genes (α1, 2; β1, 2; γ1, 2, 3). AMPK is activated typically, but not exclusively, by an increase in the AMP:ATP ratio. The enzymes regulated by AMPK include key regulators of protein, fatty acid, and glycerolipid syntheses, such as the mammalian homolog of target of rapamycin (mTOR), acetyl-CoA carboxylase (ACC), the transcriptional regulator sterol-regulatory-element-binding-protein 1C (SREBP-1C), and fatty acid synthase (FAS). Once activated, AMPK switches on ATP-producing catabolic pathways (such as fatty acid oxidation and glycolysis) and switches off ATP-consuming anabolic pathways (such as protein and fatty acid synthesis), both by short-term effects on phosphorylation and by long-term effects on gene expression. Conversely, when AMPK activities are reduced, fatty acid and protein biosynthetic pathways are activated through multiple mechanisms, including dephosphorylation of ACC and phosphorylation of ribosomal protein S6 through the mTOR signaling pathway.

Here we have examined the metabolic status of *FH*-deficient HLRCC kidney cancer tumor tissues and two distinct HLRCC kidney cancer cell lines, focusing on the aerobic glycolysis of *FH*-deficient cells, and associated changes in AMPK, HIFα subunits, and iron metabolism.

RESULTS

Glycolytic and Tumorigenic Features of *FH*-Deficient Cells Were Reversed by Restoration of *FH* Activity

We measured the levels of TCA cycle metabolites in UOK262 cells and found that fumarate levels were markedly increased, and malate levels were correspondingly low in UOK262 compared with HK-2 cells, consistent with *FH* dysfunction (Figure 1A), and these abnormalities were reversed by stable transfection of wild-type *FH* in UOK262 (UOK262-WT) (Figure 1A). To examine tumorigenicity of the HLRCC cell line, UOK262 cells were injected subcutaneously into nude mice. Palpable tumors developed within 32 days, with a tumor doubling time of ~17 days. Animals injected with UOK262-WT did not develop tumors (Figure 1B), indicating that *FH* dysfunction was required for tumor growth. We measured oxygen consumption and lactate production in UOK262 cells (Sudarshan et al., 2009; Yang et al., 2010) and in a recently derived HLRCC cell line, UOK268. Consistent with a metabolic switch to glycolytic metabolism, we observed low oxygen consumption rates and high lactate production in both UOK262 and UOK268 cells compared with HK-2 cells (Figure 1C). In addition, UOK262 cells displayed low complex I activities (Figure 1D), and electron microscopy studies revealed swollen mitochondria with severe fragmentation of the cristae in UOK262 cells, similar to abnormalities found in non-HLRCC renal cells (UOK117C4 and 786-0WT) exposed to 3-NPA, an inhibitor of the TCA cycle enzyme SDH (Figure 1E). In contrast to most other types of genetically defined kidney cancers, we observed that metastatic HLRCC kidney tumors nearly uniformly exhibit intense fluorodeoxyglucose uptake on PET scan (Figure 1F), consistent with the increased dependence on glycolysis observed in HLRCC cell lines in vitro.

Evidence for Glycolysis-Associated Cytosolic Iron Deficiency in *FH*-Deficient RCC

Recent studies have suggested that IRPs, cytosolic proteins that sense iron levels and regulate transcripts containing iron-responsive elements (IREs) (Muckenthaler et al., 2008; Rouault, 2006), are important in tumorigenesis (Maffettone et al., 2010; Zhang et al., 2008). When cytosolic iron levels are low, binding of IRPs to IREs in the 5′UTR of transcripts represses translation, whereas binding to IREs in the 3′UTR generally stabilizes the transcripts. When cytosolic iron levels are high, IRPs do not bind to IREs (Figure 2A). IRE-binding activities of IRPs were markedly higher in UOK262 cells than in control cells (Figure 2B), suggesting that cytosolic iron levels were lower in UOK262 cells. Quantitative RT-PCR showed that transcript levels of *IRP1* and *IRP2* were not increased in UOK262 cells (not shown). Increased IRP1 activities in UOK262 cells correlated with decreased cytosolic aconitase activities (Figure 2C), consistent with the conversion of IRP1 to the IRE-binding form in iron-deficient cells. Increased IRP2 activity in UOK262 cells correlated with the stabilization of IRP2 protein in iron-deficient cells (Figure 2D). Levels of the IRP target, TfR1, were higher in UOK262 cells (Figure 2E), consistent with activation of IRPs. Fumarate accumulation did not account for the increased levels of IRP2 (Figures S1A and S1B, available online).

Because UOK262 cells depend on high glucose for growth (Yang et al., 2010), these cells were routinely cultured in media containing 25 mM D-glucose (normal serum glucose: 4-6 mM). Interestingly, activation of IRPs decreased in UOK262 cells cultured in lower levels of glucose, whereas changes in glucose concentrations did not affect IRP activities and IRP2 stability in non-HLRCC cells, suggesting that features of the glycolytic

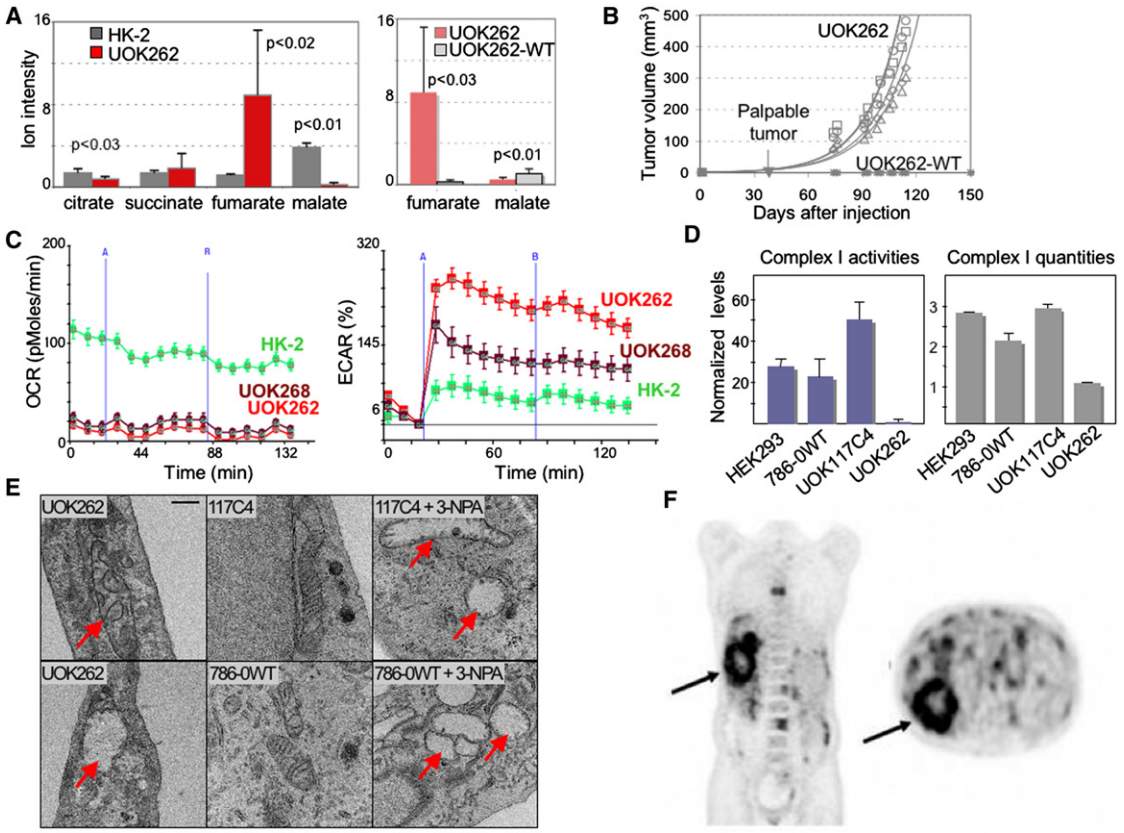

Figure 1. Mutations in *FH* compromised TCA cycle function and drove an oncogenic shift to aerobic glycolysis

(A) GC/MS analysis of TCA cycle intermediates (+/− SD) in HK-2, UOK262, and UOK262-WT cells.

(B) Growth curves of UOK262 and UOK262-WT xenografts in nude mice (n = 10 for each group) as assessed by tumor volume.

(C) Oxygen consumption rates (OCR) and extracellular acidification rates (ECAR, an indicator of glycolytic rate) in UOK262 and UOK268 cells compared with HK-2 cells upon changes from 0.5 mM to 25 mM glucose. The vertical blue lines A and B signify the time at which 25 mM glucose was infused. The ECAR plots were shown in percentage to demonstrate the fold enhancement in response to 25-mM glucose infusion.

(D) Respiratory complex I activity and protein levels (+/− SD) in UOK262 cells. Results from non-HLRCC renal cell lines, HEK293, 786-0WT, and UOK117C4, are presented as fold-differences compared with those of UOK262 cells.

(E) Electron microscopy of mitochondrial morphology (arrows) in UOK262 cells and in non-HLRCC cells (UOK117C4 and 786-0WT) treated with the SDH inhibitor, 3-NPA. Scale bar represents 0.5 μm.

(F) Positron emission tomography (PET) with fluorodeoxyglucose (^{18}FDG) in an HLRCC patient with advanced RCC demonstrated glucose uptake (black) in multiple metastases (arrow points to a representative hepatic metastasis).

All data are representative of 3 or more independent experiments. Statistical analyses were performed by Student's t test for paired samples. See also Table S1.

shift were responsible for the activation of IRPs in UOK262 cells (Figures 2F and 2G; Figures S1C–E).

Contribution of Cytosolic Iron Deficiency to Misregulation of HIFα Proteins in *FH*-Deficient RCC

Changes in cytosolic iron levels and IRP activities can potentially have competing effects on HIF-1α and HIF-2α levels. Because PHDs require iron for their enzymatic activities, decreased cellular iron levels would be expected to diminish the degradation of HIF-1α and HIF-2α proteins (Bruick and McKnight, 2001; Epstein et al., 2001). We observed that HIF-1α protein levels were markedly elevated in HLRCC tumor specimens (Figure 3A), in agreement with previous reports (Isaacs et al., 2005; Pollard et al., 2005). Similarly, HIF-1α protein levels were higher UOK262 cells (Figure 3B) and UOK268 cells (Figure 3C) compared with non-HLRCC renal cells. Fumarate accumulation was previously shown to inhibit PHDs (Isaacs et al., 2005; Pollard et al., 2005). However, our results suggest that an additional mechanism may drive the increase of HIFα in HLRCC: reduced cytosolic iron levels (as evidenced by activation of IRPs) may further stabilize HIFα proteins by inhibiting PHD activities. Furthermore, iron starvation would be expected to have different effects on expressions of the two HIFα subunits, because previous studies have shown that the HIF-2α transcript contains an IRE in its 5′UTR, and translation of the HIF-2α transcript is repressed by IRPs when cytosolic iron levels decrease (Sanchez et al., 2007; Zimmer et al., 2008). We observed that HIF-2α levels were elevated in mouse embryonic fibroblasts (MEFs) that lacked IRP1 (Figure 3D), indicating that translational repression by activated IRP1 contributes significantly to the regulation of HIF-2α levels under both iron replete and iron-depleted conditions. UOK262 cells exhibited low HIF-2α protein levels

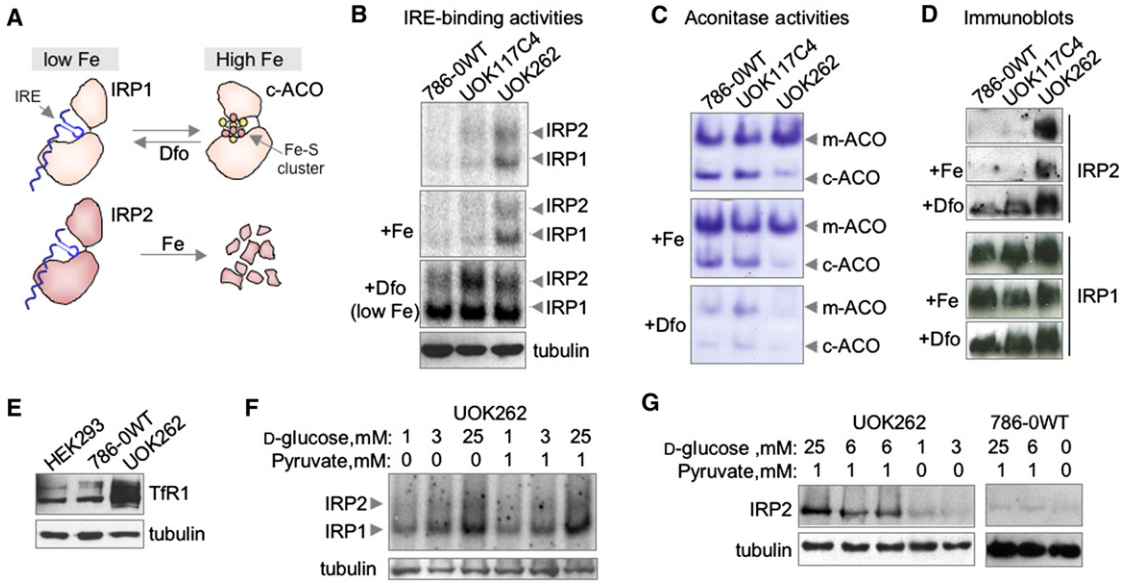

Figure 2. Evidence for glycolysis-associated cytosolic iron deficiency and IRP activation in *FH*-deficient cancer cells

(A) Schematics for iron-dependent regulation of IRP1 and IRP2. When iron is abundant, IRP2 is degraded, whereas IRP1 is converted to cytosolic aconitase (c-ACO). When iron is scarce, IRP2 is stabilized, whereas IRP1 loses its Fe-S cluster, and both IRPs bind to IREs with high affinity.

(B) IRP activities in UOK262 and non-HLRCC cells (786-0WT and UOK117C4) cultured for 16-20 hr with or without 50 uM deferoxamine (Dfo) or 100 ug/mL ferric ammonium citrate as assessed by gel-shift assays. Immunoblots of tubulin were used as loading controls.

(C) Mitochondrial and cytosolic aconitase (m-ACO and c-ACO) activities in UOK262 and non-HLRCC cells (786-0WT and UOK117C4) were assessed by in-gel aconitase activity assays.

(D) Immunoblots of IRP1 and IRP2 proteins in UOK262 and non-HLRCC cells (786-0WT and UOK117C4).

(E) Immunoblots of TfR1 in HEK293, 786-0WT, and UOK262 cells.

(F) IRP activities in UOK262 cells cultured with different glucose and pyruvate levels for 48 hr.

(G) Immunoblots of IRP2 protein in UOK262 cells and 786-0WT cells cultured in different concentrations of D-glucose.

See also Figure S1.

(Figure 3B), but not mRNA (Figure 3E) levels in both iron-replete and iron-depleted conditions, consistent with translational repression by activated IRPs. Similarly, UOK268 cells exhibited high HIF-1α and low HIF-2α protein levels (Figure 3C). These results suggested that IRP-mediated repression of HIF-2α translation selectively attenuated the increase in HIF-2α that was partly driven by iron starvation, whereas HIF-1α expression was unaffected by IRP activation (Figure S2).

Reduced AMPK Levels Resulted in Activation of Anabolic Factors and Activation of IRPs in UOK262 Cells

To understand how a mitochondrial TCA cycle dysfunction can result in changes in two cytosolic iron-sensing proteins, we examined signaling pathways that are important in metabolic adaptations. We observed that AMPKα-p levels were lower in HLRCC renal tumor specimens compared with normal kidney tissue (Figure 4A). Levels of AMPKα, AMPKβ1, phosphorylated AMPKα (AMPKα-p), phosphorylated ACC (ACC-p, an AMPK effector), and phosphorylated Akt were also low in UOK262 cells compared with several non-HLRCC kidney cell lines (HK-2, HEK293, 786-0WT) (Figure 4B), suggesting that the increased glycolysis in *FH*-deficient cancer cells did not result from activation of AMPK or Akt (Elstrom et al., 2004; Marsin et al., 2000). Quantitative RT-PCR indicated that levels of *AMPKα1* and *AMPKβ1* transcripts were relatively low in UOK262 cells (Figure 4C). Notably, the AMP:ATP ratio in UOK262 cells was comparable with HK-2 cells (Figure 4D), suggesting that the decrease in AMPKα-p levels in UOK262 cells was not caused by changes in the AMP:ATP ratio. Because low AMPK activity would be expected to decrease phosphorylation of ACC and to activate mTOR, we evaluated these AMPK targets. We observed reduced levels of ACC-p (Figure 4B), which would be expected to increase the synthesis of the key fatty acid biosynthetic intermediate, malonyl-CoA. In addition, we observed constitutive activation of the ribosomal protein S6, an mTOR downstream effector (Zhang et al., 2003) (Figure 4E). These results suggested that reduced AMPK levels might promote growth in *FH*-deficient renal cancer cells by enhancing fatty acid and protein biosynthesis (Luo et al., 2005; Menendez and Lupu, 2007).

We asked if reduced AMPK levels could activate IRPs by examining non-HLRCC cells that were treated with the AMPK inhibitor, AraA (Musi et al., 2001), or the AMPK activators, metformin and AICAR. Treatment with AraA reduced the levels of AMPKα-p and increased IRP activities (Figure 4F), whereas treatment with metformin or AICAR decreased IRP activities (Figures 4G and 4H), revealing a role of AMPK in the regulation of intracellular iron metabolism in mammalian cells. Notably, AMPKα-deficient MEFs that are deficient in both AMPKα1 and AMPKα2 (Laderoute et al., 2006) exhibited increased levels of IRP2 compared with wild-type MEFs (Figure 4I), further indicating that AMPK levels affect IRP expression.

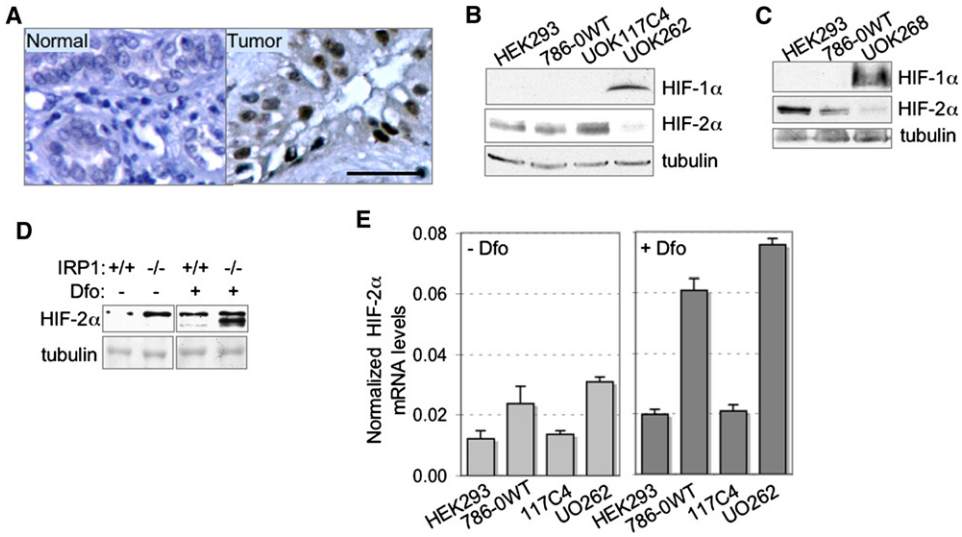

Figure 3. Contribution of cytosolic iron deficiency and IRP activities to the misregulation of HIFα proteins in *FH*-deficient cells

(A) Immunohistochemistry of HIF-1α (dark brown staining) in healthy kidney tissue and HLRCC renal tumors. Scale bar represents 30 μm.

(B) Immunoblots of HIF-1α and HIF-2α in UOK262 compared with HEK293, 786-0WT and UOK117C4 cells.

(C) Immunoblots of HIF-1α and HIF-2α in UOK268 compared with HEK293 and 786-0WT cells.

(D) Immunoblots of HIF-2α in IRP1+/+ and IRP1−/− MEF grown in normal media or treated with iron chelator DFO.

(E) *HIF-2α* mRNA levels (+/− SD) in iron-replete (-Dfo) or iron-depleted (+Dfo) HEK293, 786-0WT, UOK117C4, and UOK262 cells as assessed by qRT-PCR. Data were normalized to actin expression.

See also Figure S2.

AMPK Modulates IRP Activities through the DMT1 Iron Transporter

Although IRP1 and IRP2 activities can be differentially regulated by many factors (Rouault, 2006), the most likely cause for simultaneous activation of both IRPs is cytosolic iron depletion. We observed that the protein levels of DMT1 (Tabuchi et al., 2002), which transport iron from the endosome into the cytosol after iron uptake via TfR1 (Mims and Prchal, 2005), were extremely low in UOK262 cells (Figure 5A). *DMT1* transcript levels in UOK262 cells were 2-10 fold lower compared with non-HLRCC cells (Figure S3). Iron depletion with Dfo did not significantly increase DMT1 levels in UOK262 cells, unlike in HEK293 and UOK117C4 cells (Figure 5B). These results suggested that reduced iron uptake through DMT1 caused the activation of IRPs in UOK262 cells.

To determine whether the changes of AMPK and DMT1 observed in UOK262 cells were driven by loss of *FH*, we compared the levels of these proteins in UOK262 and UOK262-WT cells. Expression of wild-type *FH* in UOK262 cells increased the levels of DMT1 and AMPKα (Figure 5C), suggesting that the observed decreases in AMPKα and DMT1 levels were attributable to the loss of functional *FH* in UOK262 cells. Furthermore, activation of AMPK in UOK262 cells by glucose limitation was accompanied by an increase in DMT1 levels (Figure 5D), and increased iron uptake through DMT1 likely accounted for the reduced activation of IRPs in UOK262 cells grown in low glucose (Figures 2F and 5D).

We asked whether reduced AMPK levels could lead to a reduction of DMT1 levels and thereby activate IRPs in UOK262 cells by evaluating the response of non-HLRCC cells to treatment with either the AMPK activator, metformin, or the AMPK inhibitor, AraA. Treatment of 786-0WT cells (Figure 5E) and UOK117C4 cells (data not shown) with metformin increased ACC-p and DMT1 levels and decreased IRP activities, whereas treatment with AraA concomitantly reduced AMPKα-p levels and DMT1 expression (Figure 5F). In addition, AMPKα-deficient MEFs exhibited lower levels of DMT1 and increased levels of IRP2 compared with wild-type MEFs, further suggesting that AMPK levels regulate IRP activities through changes in DMT1 expression (Figure 5G).

Recently, induction of p53 was shown to decrease IRP activities (Zhang et al., 2008), but the mechanism was unknown. We observed that UOK262 cells had very low p53 levels (Figure 5H), consistent with our observation that AMPK is low in UOK262 cells and reports that AMPK stabilizes p53 through phosphorylation (Imamura et al., 2001; Jones et al., 2005). To assess the role of p53 in IRP activation, we showed that induction of p53 increased DMT1 levels in p53ind cells (Figure 5I), whereas control cells transfected with an empty vector exhibited no change in DMT1 levels (data not shown). Conversely, siRNA-mediated silencing of p53 in HEK293 cells decreased DMT1 levels (Figure 5J). These results suggested that AMPK may regulate DMT1 expression in part through its effect on p53 levels.

FH-Deficient UOK268 Cells also Displayed Reduced Levels of AMPK, p53, and DMT1, and Stabilization of IRP2

To further confirm the significance of *FH*-AMPK-DMT1-IRP pathway in HLRCC tumors, we examined UOK268 cells. Similar to UOK262 cells, UOK268 cells displayed reduced levels of AMPKα-p, ACC-p, AMPKα, AMPKβ1, and p53 (Figure 6A–C). We observed that DMT1 levels were low and IRP2 levels were

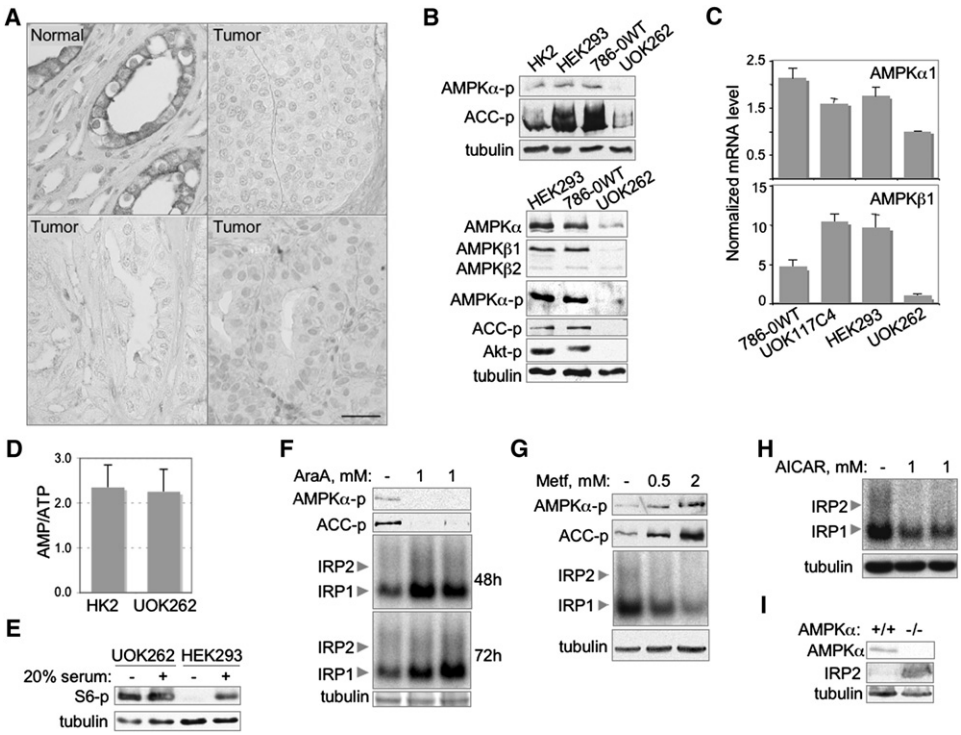

Figure 4. Reduced AMPK levels resulted in activation of anabolic factors ACC and S6, and activation of IRPs in UOK262 and control cells

(A) Levels of AMPKα-p (T172) in healthy kidney tissue and in renal tumors from three patients with HLRCC-associated kidney cancer were assessed by immunohistochemistry (blue-black). Nuclei were stained with Methyl green. Scale bar represents 30 μm.

(B) Immunoblots of AMPKα-p (T172), ACC-p (S79) (upper panel) and AMPKα, AMPKβ, Akt-p (S473) (lower panel) in UOK262 compared with non-HLRCC cells (HK2, HEK293, and 786-0WT).

(C) Levels of *AMPKα1* and *AMPKβ1* transcripts (+/− SD) in 786-0WT, UOK117C4, HEK293, and UOK262 cells were assessed by qRT-PCR. Data were normalized with actin transcript levels and presented as fold-differences compared with those of UOK262 cells.

(D) GC/MS analysis of the AMP:ATP ratio in UOK262 cells and control HK-2 cells.

(E) Immunoblots of S6-p (an mTOR downstream effector) in cells that were serum-starved (0.5% serum) for 2 days and then stimulated with 20% serum for 30 min.

(F) Immunoblots of AMPKα-p, ACC-p, and IRP activities in 786-0WT cells that were cultured with or without AraA for 48 hr or 72h.

(G) Immunoblots of AMPKα-p, ACC-p, and IRP activities in 786-0WT cells that were cultured with or without metformin (Metf) for 72 hr.

(H) IRP activities in 786-0WT cells treated with the AMPK activator AICAR for 72 hr.

(I) Immunoblots of IRP2 in AMPKα-deficient MEFs compared with wild-type MEFs.

high in UOK268 compared with control cells (Figure 6A). These results from a second HLRCC cell line confirmed that remodeling of the AMPK pathway and intracellular iron homeostasis is reproducible in *FH*-deficient RCC cell lines.

Key Elements of the Metabolic Profile of *FH*-Deficient Cells can Be Recapitulated by Chemical Inhibition of the TCA Cycle

Next, we asked whether inhibition of other TCA cycle enzymes induced changes in AMPK, DMT1, and IRPs similar to those observed in *FH*-deficient cells. Treatment with 2-thenoyltrifluoroacetone (TTFA), which inhibits SDH at the SDHD subunit (Sun et al., 2005), resulted in increased IRP activities (Figure 7A) and increased IRP2 and TfR1 protein levels (Figure 7B) in three different non-HLRCC cell lines. As shown in Figure 2F, IRP activation in UOK262 cells was glucose-dependent. Similarly, increasing glucose concentrations increased the TTFA-dependent activation of IRPs (Figure 7C and D), whereas lowering glucose concentrations abolished the effect of TTFA on IRP activities (Figure 7C). Thus, inhibition of SDH activity by TTFA recapitulated the IRP activation observed in *FH*-deficient cells.

Previous studies have shown that mitochondrial inhibitors can have biphasic effects on AMPKα phosphorylation (Figure S4A). Similarly, we observed that TCA cycle inhibition of non-HLRCC cells with TTFA initially resulted in a rapid decrease in ATP levels (Figure 7E) and a corresponding transient increase in AMPKα-p (0.25h) (Figure 7F), followed by a partial recovery of ATP levels (probably as a result of increased aerobic glycolysis) (Figure 7E) and a decrease in AMPKα–p and AMPKα protein levels at later time-points (Figure 7F). At the 48-h time point, there were overall decreases in AMPKα and AMPKα-p levels, with corresponding decrease in ACC-p and p53 levels, and increase in S6-p levels (Figure 7G). More importantly, the long-term TTFA-mediated decrease in AMPK levels correlated with diminished DMT1 levels and increased IRP activities in both HEK293 and UOK117C4 cells (Figure 7H). In addition to TTFA, treatment with inhibitors to other SDH subunits (3-NPA) and aconitase ($MnCl_2$) also led to reduced AMPKα-p levels and DMT1 expression, and

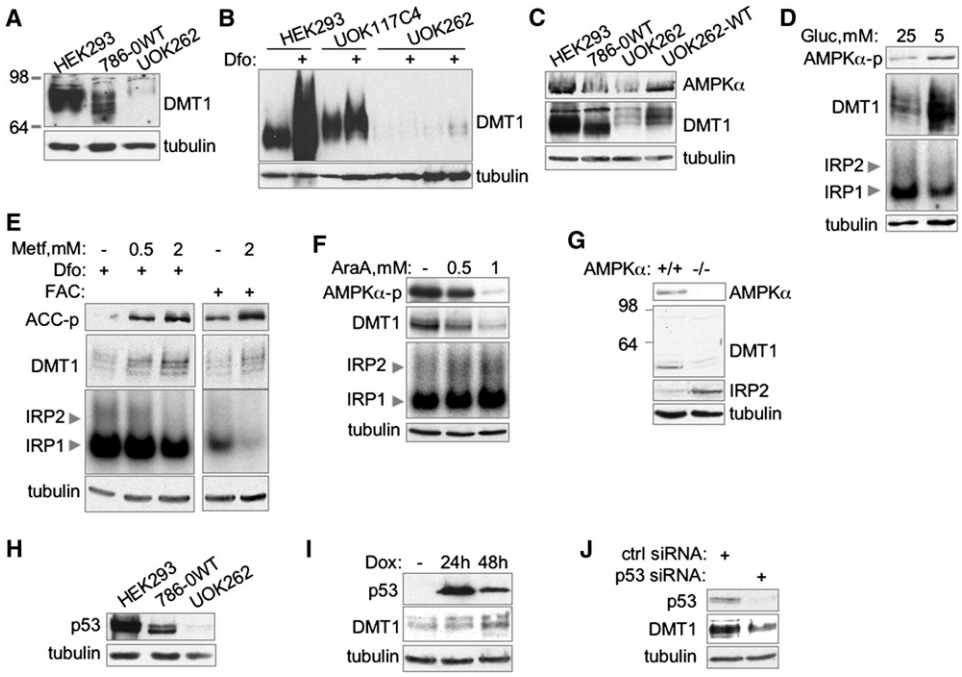

Figure 5. Reduced AMPK levels in UOK262 cells diminished the expression of the iron transporter DMT1, resulting in activation of IRPs

(A) Immunoblots of DMT1 (glycolysated forms at 70-100kDa) in UOK262 cells compared with HEK293 and 786-0WT cells.

(B) Immunoblots of DMT1 in HEK293, UOK117C4, and UOK262 cells that were treated with iron chelator Dfo for 16 hr.

(C) Comparison of AMPKα and DMT1 levels in HEK293, 786-0WT, UOK262, and UOK262-WT cells.

(D) Immunoblots of AMPKα-p and DMT1, and IRP activities in UOK262 cells cultured in different concentrations of glucose for 48 hr.

(E) Immunoblots of ACC-p and DMT1, and IRP activities in 786-0WT cells treated with metformin (72 hr), Dfo (16 hr), and/or FAC (16 hr).

(F) Immunoblots of AMPKα-p and DMT1, and IRP activities in 786-0WT cells treated with AraA for 48 hr.

(G) Immunoblots of AMPKα, DMT1 (unglycolysated form at ~55 kDa) and IRP2 in AMPKα-deficient MEFs compared with wild-type MEFs.

(H) Immunoblots of p53 in UOK262 cells compared with HEK293 and 786-0WT cells.

(I) Effect of increased expression of p53 (induced by doxycycline treatment of p53ind cells) on DMT1 protein levels.

(J) Effect of siRNA-mediated silencing of p53 on the levels of DMT1 in HEK293 cells.

See also Figure S3.

increased IRP activities (Figure S4). Thus, chemical disruption of the TCA cycle can cause non-cancer cells to remodel their metabolism to include decreased AMPK and DMT1 levels and activation of IRPs, similar to *FH*-deficient UOK262 and UOK268 cells.

Silencing of HIF-1α and Activation of AMPK Reduced the Tumorigenic Potential of UOK262 Cells

Previous studies have shown that elevation of HIF-2α is essential for tumor growth of Von Hippel-Lindau (VHL)-deficient cells in xenograft mouse models (Kondo et al., 2002; Maranchie et al., 2002). Therefore, we compared HIFα levels in UOK262 cells (a papillary type 2 RCC) with 786-0 cells (a VHL-deficient clear cell RCC) (Figure 8A). In contrast to UOK262 cells, 786-0 cells exhibited very low levels of HIF-1α and high levels of HIF-2α. Compared with 786-0 cells, UOK262 cells also exhibited decreased AMPKα-p, AMPKβ1, and DMT1 levels, and increased IRP2 levels. These distinctions between VHL-deficient and *FH*-deficient cells suggest that disease-specific therapies could be developed. Specifically, we observed that siRNA-mediated silencing of HIF-1α (Figure 8B) or activation of AMPK using metformin and AICAR (Figure 8C) markedly inhibited invasion activities of UOK262 cells, suggesting that modulation of HIF-1α and AMPK signaling may offer opportunities for targeted therapeutic approaches to the treatment of patients with HLRCC-associated kidney cancer.

DISCUSSION

Fumarate hydratase-deficient kidney cancer, a clear example of the Warburg effect in cancer, is an unusually aggressive form of type 2 papillary kidney cancer that metastasizes when the primary tumors are as small as 1 cm, and is nearly uniformly fatal once it has spread beyond the kidney. Here, we showed that HLRCC tumors and two different *FH*-deficient RCC cell lines depended on glycolysis and had low AMPK levels. In addition to promoting fatty acid and protein biosynthetic pathways (through the activation of ACC and S6), low AMPK levels reduced the expression of DMT1 and activated IRP1 and IRP2 (Figure 8D). Our studies demonstrated that p53 enhances expression of DMT1 (Figure 5I), and the AMPK-dependent reduction of p53 would thus be expected to cause cytosolic iron deficiency, activation of IRPs, and translational repression of the iron-storage protein ferritin. Previous studies have shown that synthesis of ferritin is decreased in cells that are stimulated by several oncogenes (Tsuji et al., 1995; Wu et al., 1999). Our

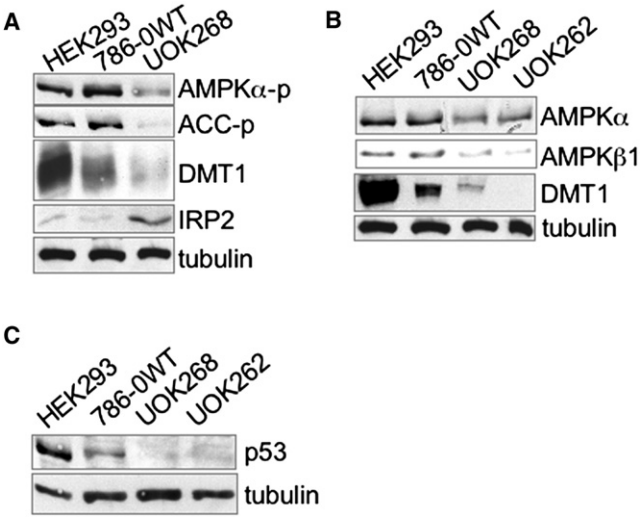

Figure 6. A second glycolytic HLRCC cancer cell line, UOK268, exhibited decreased levels of AMPK, DMT1 and p53

(A) Immunoblots of AMPKα-p, ACC-p (an AMPK effector), DMT1, and IRP2 in UOK268 compared with HEK293 and 786-0WT cells.

(B) Immunoblots of AMPKα, AMPKβ, and DMT1 levels in UOK268 cells compared with HEK293, 786-0WT, and UOK262 cells.

(C) Immunoblots of p53 in UOK268 compared with HEK293, 786-0WT, and UOK262 cells.

studies demonstrated that an induction of p53 resulted in increased expression of DMT1 (Figure 5I), providing one mechanism for the previously reported p53-dependent decrease in IRP activities and increase in ferritin levels (Zhang et al., 2008). In respiring cells, DMT1 expression is important for the uptake of iron for the biosynthesis of heme and Fe-S cluster cofactors in the mitochondrial respiratory complexes. The AMPK-dependent decrease of DMT1 levels may represent an integral part of the metabolic shift to glycolysis, because less iron may be needed to support energy metabolism in glycolytic cells compared with respiring cells. In addition, when cells are required to produce energy from glycolysis, low iron levels may consolidate the shift to glycolysis by stabilizing HIF-1α or other participants in the remodeled metabolism of *FH*-deficient cells.

Previous studies have shown that elevation of HIFα levels in *FH*-deficient cells resulted from fumarate accumulation, which inhibits the PHDs that mark HIFα proteins for degradation (Isaacs et al., 2005; Pollard et al., 2005). However, many other factors may also contribute to *FH*-associated neoplasias. We suggest that HIF1α is increased in HLRCC in part because cytosolic iron deficiency also inhibits PHD activities and contributes to the stabilization of HIF-1α proteins. Furthermore, because the HIF-2α transcript contains an IRE in its 5′UTR (Sanchez et al., 2007), whereas the HIF-1α transcript does not, activation of IRPs would be expected to selectively repress HIF-2α translation. We suggest that IRP activation explains why HIF-1α levels were markedly elevated, whereas HIF-2α protein levels were very low in UOK262 and UOK268 cells (Figure 3B and 3C), even though HIF-2α transcript levels in UOK262 cells were comparable with control cells (Figure 3E).

The differential expression levels of HIFα proteins in 786-0 and UOK262 cells (Figure 8A) have important implications for the development of targeted therapeutic treatment of VHL-deficient and *FH*-deficient RCC. Although HIF-1α has been shown to promote tumorigenesis in colon and pancreatic cancer cells (Chen et al., 2003; Dang et al., 2006), studies in RCC have shown that activation of HIF-2α, and not HIF-1α, is necessary for the tumorigenesis of VHL-deficient RCC (Kondo et al., 2002; Maranchie et al., 2002). HIF-1α and HIF-2α have both overlapping as well as distinct targets (Gordan and Simon, 2007; Kaelin and Ratcliffe, 2008; Raval et al., 2005), and HIF-1α is uniquely involved in activating genes associated with glycolysis (Gordan and Simon, 2007; Haase, 2010). In this study, we showed that silencing of HIF-1α inhibited the invasion activities of UOK262 cells (Figure 8B), further suggesting that elevation of HIF-1α is critical for engineering the switch to glycolytic metabolism in UOK262 cells.

Notably, the coordination that we observed here between glucose and iron metabolisms in *FH*-deficient RCC has an evolutionary precedent in the metabolism of *Saccharomyces cerevisiae*. When grown in glucose-rich medium, *S. cerevisiae* uses fermentation (a microbial equivalent of glycolysis) as its main metabolic pathway, and repression of the yeast AMPK homolog, SNF1, represses expression of iron uptake genes (Haurie et al., 2003). As glucose concentrations decrease, activation of SNF1 induces expression of iron uptake genes and facilitates the shift to oxidative metabolism. Conversely, iron deficiency in *S. cerevisiae* results in phosphorylation of SNF1, which increases glucose uptake and glycolysis, allowing the cells to switch from respiratory to fermentative metabolism (Puig et al., 2008). Our results suggest that the high glycolytic flux in UOK262 cells reduces AMPK and DMT1 expression levels, whereas glucose depletion diminished glycolysis and increased AMPK signaling and DMT1 expression (Figure 5D). These studies suggest that AMPK/SNF1 signaling provides an evolutionarily conserved linkage between intermediary metabolism and intracellular iron homeostasis. Interestingly, although the activities of several Fe-dependent enzymes, including respiratory complex I and cytosolic aconitase, were low in UOK262 cells (Figure 1D and 2C), mitochondrial aconitase activities were not diminished in UOK262 cells (Figure 2C), suggesting that these cells can preferentially direct iron to specific proteins or pathways.

Although previous studies on AMPK signaling have largely focused on the increase in AMPKα phosphorylation and its role in increasing catabolism during the acute response to metabolic stress (Hardie, 2007), fewer studies have characterized the potential importance of low AMPK activity in promoting activities of anabolic pathways in tumorigenesis (Jones and Thompson, 2009; Luo et al., 2005; Shaw, 2006). Here, we not only showed that levels of AMPKα-p were diminished in *FH*-deficient cells, but we also found that AMPK signaling was also regulated at the transcript and/or protein levels (Figure 4B and 4C). This metabolic remodeling was not unique to *FH*-deficient cells, because chemical inhibition of SDH in non-cancer cells also resulted in reduced levels of AMPK, p53, ACC-p, and DMT1, and increased levels of S6-p (Figure 7). Time-course studies indicated that, upon chemical inhibition of SDH, changes of AMPK activities inversely correlated with changes in intracellular ATP levels: ATP levels decreased initially upon SDH inhibition, and

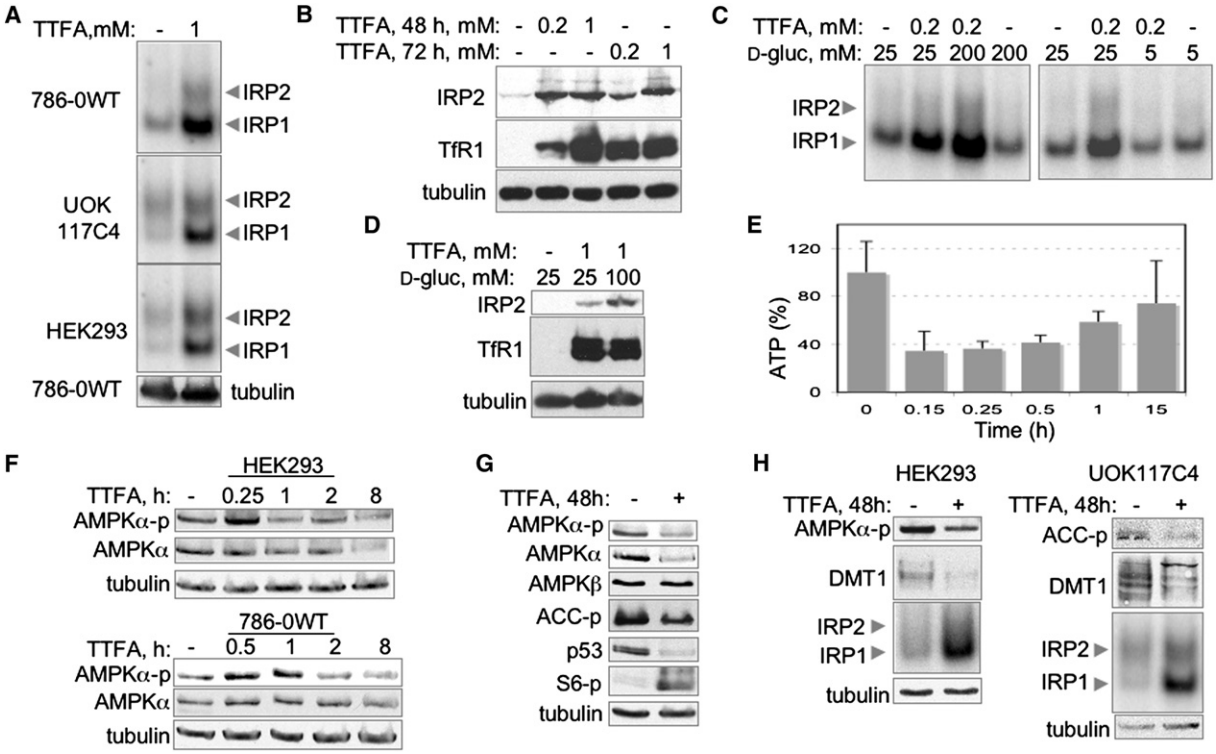

Figure 7. Chemical inhibition of SDH in non-HLRCC cells can induce metabolic changes similar to those observed in *FH*-deficient UOK262 cells

(A) IRP activities were assessed in 786-0WT, UOK117C4, and HEK293 cells that were treated with TTFA, an inhibitor of SDH, for 48 hr.

(B) Immunoblots of IRP2 and TfR1 in 786-0WT cells treated with TTFA.

(C) IRP activities in 786-0WT cells treated with TTFA at different glucose concentrations.

(D) Immunoblots of IRP2 and TfR1 in 786-0WT cells treated with TTFA at different glucose concentrations.

(E) Time-dependent effect of 1 mM TTFA treatment on ATP levels (+/− SD) in HEK293 cells.

(F) Time-dependent effect of 1 mM TTFA treatment on the levels of AMPKα and AMPKα-p in HEK293 and 786-0WT cells as assessed by immunoblot analysis.

(G) Effect of TTFA treatment for 48 hr on the levels of AMPKα-p, AMPKα, AMPKβ, ACC-p, p53, and S6-p in HEK293 cells.

(H) Effect of TTFA treatment of HEK293 and UOK117C4 cells for 48 hr on the levels of AMPKα-p, ACC-p, DMT1, and IRP activities.

See also Figure S4.

then gradually recovered over the following hours (Figure 7E), whereas after an initial rapid increase, AMPKα-p levels dropped below the levels of untreated cells (Figure 7F). After a 48-hr treatment with TTFA, there was also a marked decrease in AMPKα protein levels (Figure 7G), which further ensured that levels of AMPKα-p decreased regardless of the AMP:ATP ratio. These results are similar to the decreased levels of AMPKα-p, AMPKα, and AMPKβ1 proteins and transcripts that were observed in *FH*-deficient cells (Figures 4B and 4C), and they show that the obligate shift to glycolysis in *FH*-deficient cells produces associated changes in AMPK activity that enhance anabolic reactions.

The high glycolytic rate, together with the decrease of AMPK signaling, can provide several potential growth advantages to *FH*-deficient RCC. Although the yield of ATP per glucose molecule is higher in OXPHOS than in glycolysis, aerobic glycolysis can provide sufficient energy for cell proliferation provided the glycolytic flux is high enough (DeBerardinis et al., 2008). Aerobic glycolysis can also confer growth advantages by diverting some of the glucose into pathways that generate NADPH, acetyl-CoA, and ribose for fatty acid, protein, and nucleotide synthesis (Vander Heiden et al., 2009). Reduced AMPK activities would promote the efficient use of the NADPH, acetyl-CoA, and ribose generated by aerobic glycolysis by activating anabolic factors involved in protein and fatty acid synthesis (Hardie, 2007). Many cancers are characterized by upregulation of anabolic factors such as ACC, FAS, and mTOR, all of which are inhibited by AMPK activation (Jones and Thompson, 2009; Luo et al., 2005; Shaw, 2006). Notably, reduced AMPK phosphorylation was recently reported in breast cancer specimens (Hadad et al., 2009). Alterations in the LKB1/AMPK/TSC/mTOR pathway are associated with a wide variety of cancers and hamartomas, including Peutz-Jeghers syndrome and tuberous sclerosis complex (Inoki and Guan, 2009; Jones and Thompson, 2009; Shaw, 2006). The tumor suppressor, p53, is a downstream effector of AMPK, and p53 mutations are found in 50% of all human cancers (Vousden and Ryan, 2009). Here, we established that diminished p53 levels result from AMPK-dependent metabolic remodeling, adding to the potential mechanisms that impair p53 function in tumorigenesis. Thus, the marked increase in glycolysis and reduced AMPK levels in *FH*-deficient cancer cells together may promote anabolic metabolism (through the activation of ACC and S6) and repress senescence and

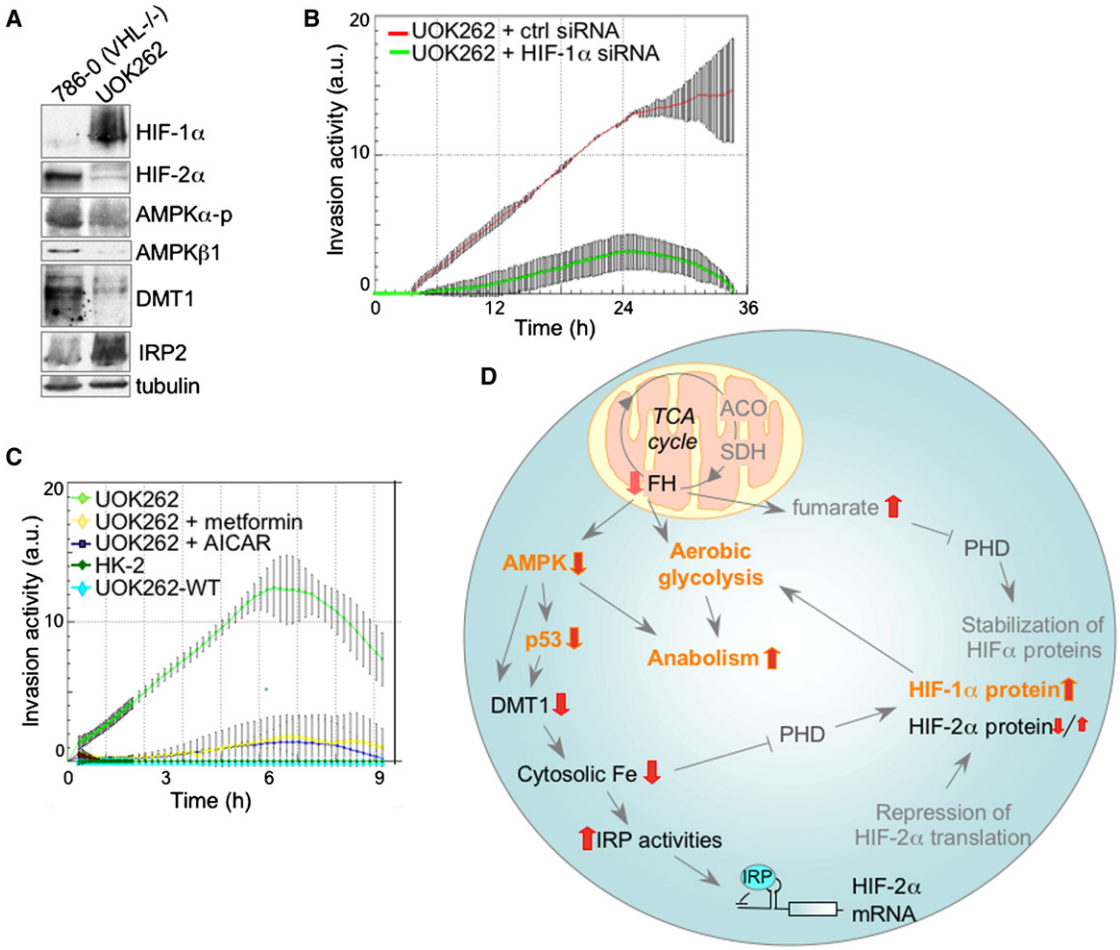

Figure 8. Silencing of HIF-1α and activation of AMPK reduced the invasive potential of the *FH*-deficient UOK262 cells, which have a distinctive metabolic profile

(A) Immunoblots of HIF-1α, HIF-2α, AMPKα-p, AMPKβ, DMT1, IRP2 in UOK262 compared with 786-0 cells.

(B) Effect of siRNA-mediated silencing of HIF-1α on the invasion activities of UOK262 cells measured using the RT-CIM cell invasion monitoring system.

(C) Effect of treatment with the AMPK activators metformin and AICAR on the invasion activities of UOK262 cells.

(D) A working model for *FH*-deficient cells, in which impairment of the TCA cycle imposes a need to shift energy production from respiration to glycolysis, and induces an AMPK-dependent decrease in p53 and activation of anabolic factors ACC and S6. Reduced AMPK levels decrease expression of the DMT1 iron transporter, resulting in reduced iron uptake and activation of IRPs. While reduced cytosolic iron levels and fumarate accumulation are expected to inhibit PHDs and stabilize both HIF-1α and HIF-2α proteins, activation of IRPs would selectively repress HIF-2α translation and attenuate the potential increase in HIF-2α proteins. The increased expression of HIF-1α and glycolytic shift, coupled to decreases of AMPK and p53 levels, and increased activity of anabolic pathways (shown in orange) may all confer growth/survival advantages to *FH*-deficient RCC.

apoptosis (as a result of the decrease of p53 levels) (Vousden and Ryan, 2009) in a manner conducive to cancer cell proliferation (Figure 8D).

Our demonstration that metformin and AICAR reduced the invasion activities of UOK262 cells (Figure 8C) is consistent with previous studies that showed that metformin and AICAR inhibited the proliferation of various cancer cell lines (Buzzai et al., 2007; Hirsch et al., 2009; Xiang et al., 2004), and that diabetics treated with metformin exhibited decreases in cancer incidence (Evans et al., 2005). Metformin can inhibit tumorigenesis by activating AMPK, and thereby inhibiting anabolic pathways (Shaw, 2006) and inducing apoptosis (Buzzai et al., 2007). However, our findings also suggest another potential mechanism for the anti-cancer effect of metformin: induction of DMT1 expression (Figure 5E) may increase iron uptake, which may reduce HIF-1α levels and associated glycolysis, while promoting oxidative damage to DNA, proteins, and lipids in cancer cells.

Interest in the Warburg effect (Vander Heiden et al., 2009; Warburg, 1956) has been rekindled by the mounting appreciation for the growth advantages that glycolysis can confer to tumor cells (Shaw, 2006; Vander Heiden et al., 2009; Warburg, 1956). In neoplasia, oncogenic pathways may function to drive cell-autonomous nutrient uptake and anabolic metabolism via aerobic glycolysis (Vander Heiden et al., 2009). We propose that the AMPK-dependent decrease in iron uptake in *FH*-deficient cells reflects a reversion to an evolutionarily conserved pathway that coordinates glucose and iron metabolisms. Our results suggest that a fundamental feature of HLRCC carcinogenesis involves

reduced AMPK activities, which mediate a global remodeling of anabolic processes and iron metabolism to enhance cell proliferation and survival. The metabolic shift to aerobic glycolysis described in this aggressive form of cancer could provide insight into the most fundamental aspects of tumorigenesis and provide opportunities for the development of improved diagnostics and therapeutics in tumors characterized by aerobic glycolysis and impaired oxidative phosphorylation.

EXPERIMENTAL PROCEDURES

Cell Cultures and Animal Studies

Kidney cell lines used in this study are summarized in Table S1. p53ind and control p53- cell lines were generous gifts from the Torti lab (Wake Forest University). AMPK+/+ and AMPK−/− MEFs were generous gifts from Dr Benoit Viollet (Université Paris Descartes, CNRS). All cells were cultivated in DMEM containing 25 mM D-glucose, 1 mM pyruvate, 10% fetal bovine serum, and 2 mM L-glutamine. Embryonic fibroblasts of 13-day-old embryos were isolated from wild-type and IRP1−/− mice as previously described (LaVaute et al., 2001). For xenograft studies, UOK 262 or UK262-WT cells (5×10^6) were injected subcutaneously into 10 athymic nude mice and tumor growth was followed by measurements of tumor volume over time. All protocols were approved by the NICHD Animal Care and Use Committee and met NIH guidelines for the humane care of animals.

Immunoblots

Immunoblots were performed on 1% Triton lysate, whole-cell lysates (RIPA buffer or 4% SDS in PBS) or nuclear extracts. Equal loading was assessed by Ponceau Red staining and immunoblot with anti-tubulin or anti-CREB antibodies. Antibodies are described in supplementary information.

IRP Activity Assays

Assay samples containing 25 mM Tris-HCl (pH7.5), 40mM KCl. 5% glycerol, 0.1U/uL SuperRNAsine (Ambion, Austin, TX), 0.3 uL/uL yeast tRNA, 2.5 mM DTT and 10 nM P^{32}-labeled IRE of human ferritin H chain and 10 ug protein were loaded onto a 8% acrylamide/TBE gel and run at 200 V for 5 hr at room temperature. Equal loading was assessed by immunoblot with IRPs and anti-tubulin antibodies.

Measurements of Metabolic Status

Cells were cultured in custom XF96 microplates (Seahorse Bioscience, Chicopee, MA). Respiration and glycolysis cause rapid changes to the concentrations of dissolved oxygen and free protons in the medium above a monolayer of cells, which are measured by solid-state sensor probes in the XF96 Analyzer. Glucose (25 mM) was injected at the indicated time-points into each well after baseline rate measurement. Analysis of TCA cycle intermediates, ATP and AMP, were performed using GC/MS analyses of 6 samples by Metabolon, Inc. (Durham, NC).

Invasion Assays

RT-CIM cell invasion and migration monitoring system (ACEA Biosciences, San Diego, CA) was used to measure invasion of UOK262 cells transfected by electroporation (AMAXA) with 10 uM of HIF-1α siRNA or mock RNA, or UOK262 cells treated with 2 mM metformin or 1 mM AICAR. One-day post-transfection, cells were serum-starved overnight before being plated in the upper chambers, whereas the lower chambers contained media with 10% serum. Impedance signals from invasive cells passing through the membrane between the chambers were recorded in real-time to provide quantitative information about the number of migrating cells.

Human Materials

All human subjects work was approved by NCI Institutional Review Board Committee. Renal tumors from patients affected with HLRCC were removed surgically at the NIH. Informed consent was obtained from all subjects. Patients were evaluated on approved NCI-IRB protocols 97-C-0147 and/or 03-C-0066.

Data Analysis

All data are representative of three or more independent experiments. Statistical analyses were performed by Student's t test for paired samples.

Additional information on experimental procedures is described in the on-line supplemental information.

SUPPLEMENTAL INFORMATION

Supplemental Information includes four figures, one table, Supplemental Experimental Procedures, and Supplemental References and can be found with this article online at doi:10.1016/j.ccr.2011.07.018.

ACKNOWLEDGMENTS

The authors thank our colleagues and thank the intramural programs of the National Institute of Child Health and Human Development and the National Cancer Institute for support.

Received: September 10, 2010
Revised: January 6, 2011
Accepted: July 28, 2011
Published: September 12, 2011

REFERENCES

Bayley, J.P., and Devilee, P. (2010). Warburg tumours and the mechanisms of mitochondrial tumour suppressor genes. Barking up the right tree? Curr. Opin. Genet. Dev. *20*, 324–329.

Baysal, B.E., Ferrell, R.E., Willett-Brozick, J.E., Lawrence, E.C., Myssiorek, D., Bosch, A., van der Mey, A., Taschner, P.E., Rubinstein, W.S., Myers, E.N., et al. (2000). Mutations in SDHD, a mitochondrial complex II gene, in hereditary paraganglioma. Science *287*, 848–851.

Bruick, R.K., and McKnight, S.L. (2001). A conserved family of prolyl-4-hydroxylases that modify HIF. Science *294*, 1337–1340.

Buzzai, M., Jones, R.G., Amaravadi, R.K., Lum, J.J., DeBerardinis, R.J., Zhao, F., Viollet, B., and Thompson, C.B. (2007). Systemic treatment with the antidiabetic drug metformin selectively impairs p53-deficient tumor cell growth. Cancer Res. *67*, 6745–6752.

Chen, J., Zhao, S., Nakada, K., Kuge, Y., Tamaki, N., Okada, F., Wang, J., Shindo, M., Higashino, F., Takeda, K., et al. (2003). Dominant-negative hypoxia-inducible factor-1 alpha reduces tumorigenicity of pancreatic cancer cells through the suppression of glucose metabolism. Am. J. Pathol. *162*, 1283–1291.

Dang, D.T., Chen, F., Gardner, L.B., Cummins, J.M., Rago, C., Bunz, F., Kantsevoy, S.V., and Dang, L.H. (2006). Hypoxia-inducible factor-1alpha promotes nonhypoxia-mediated proliferation in colon cancer cells and xenografts. Cancer Res. *66*, 1684–1936.

DeBerardinis, R.J., Lum, J.J., Hatzivassiliou, G., and Thompson, C.B. (2008). The biology of cancer: metabolic reprogramming fuels cell growth and proliferation. Cell Metab. *7*, 11–20.

Elstrom, R.L., Bauer, D.E., Buzzai, M., Karnauskas, R., Harris, M.H., Plas, D.R., Zhuang, H., Cinalli, R.M., Alavi, A., Rudin, C.M., and Thompson, C.B. (2004). Akt stimulates aerobic glycolysis in cancer cells. Cancer Res. *64*, 3892–3899.

Epstein, A.C., Gleadle, J.M., McNeill, L.A., Hewitson, K.S., O'Rourke, J., Mole, D.R., Mukherji, M., Metzen, E., Wilson, M.I., Dhanda, A., et al. (2001). C. elegans EGL-9 and mammalian homologs define a family of dioxygenases that regulate HIF by prolyl hydroxylation. Cell *107*, 43–54.

Evans, J.M., Donnelly, L.A., Emslie-Smith, A.M., Alessi, D.R., and Morris, A.D. (2005). Metformin and reduced risk of cancer in diabetic patients. BMJ *330*, 1304–1305.

Gordan, J.D., and Simon, M.C. (2007). Hypoxia-inducible factors: central regulators of the tumor phenotype. Curr. Opin. Genet. Dev. *17*, 71–77.

Haase, V.H. (2010). Hypoxic regulation of erythropoiesis and iron metabolism. Am. J. Physiol. Renal Physiol. *299*, F1–F13.

Hadad, S.M., Baker, L., Quinlan, P.R., Robertson, K.E., Bray, S.E., Thomson, G., Kellock, D., Jordan, L.B., Purdie, C.A., Hardie, D.G., et al. (2009). Histological evaluation of AMPK signalling in primary breast cancer. BMC Cancer *9*, 307.

Hao, H.X., Khalimonchuk, O., Schraders, M., Dephoure, N., Bayley, J.P., Kunst, H., Devilee, P., Cremers, C.W., Schiffman, J.D., Bentz, B.G., et al. (2009). SDH5, a gene required for flavination of succinate dehydrogenase, is mutated in paraganglioma. Science *325*, 1139–1142.

Hardie, D.G. (2007). AMP-activated/SNF1 protein kinases: conserved guardians of cellular energy. Nat. Rev. Mol. Cell Biol. *8*, 774–785.

Haurie, V., Boucherie, H., and Sagliocco, F. (2003). The Snf1 protein kinase controls the induction of genes of the iron uptake pathway at the diauxic shift in Saccharomyces cerevisiae. J. Biol. Chem. *278*, 45391–45396.

Hirsch, H.A., Iliopoulos, D., Tsichlis, P.N., and Struhl, K. (2009). Metformin selectively targets cancer stem cells, and acts together with chemotherapy to block tumor growth and prolong remission. Cancer Res. *69*, 7507–7511.

Imamura, K., Ogura, T., Kishimoto, A., Kaminishi, M., and Esumi, H. (2001). Cell cycle regulation via p53 phosphorylation by a 5′-AMP activated protein kinase activator, 5-aminoimidazole- 4-carboxamide-1-beta-D-ribofuranoside, in a human hepatocellular carcinoma cell line. Biochem. Biophys. Res. Commun. *287*, 562–567.

Inoki, K., and Guan, K.L. (2009). Tuberous sclerosis complex, implication from a rare genetic disease to common cancer treatment. Hum. Mol. Genet. *18* (R1), R94–R100.

Isaacs, J.S., Jung, Y.J., Mole, D.R., Lee, S., Torres-Cabala, C., Chung, Y.L., Merino, M., Trepel, J., Zbar, B., Toro, J., et al. (2005). HIF overexpression correlates with biallelic loss of fumarate hydratase in renal cancer: novel role of fumarate in regulation of HIF stability. Cancer Cell *8*, 143–153.

Jones, R.G., Plas, D.R., Kubek, S., Buzzai, M., Mu, J., Xu, Y., Birnbaum, M.J., and Thompson, C.B. (2005). AMP-activated protein kinase induces a p53-dependent metabolic checkpoint. Mol. Cell *18*, 283–293.

Jones, R.G., and Thompson, C.B. (2009). Tumor suppressors and cell metabolism: a recipe for cancer growth. Genes Dev. *23*, 537–548.

Kaelin, W.G., Jr., and Ratcliffe, P.J. (2008). Oxygen sensing by metazoans: the central role of the HIF hydroxylase pathway. Mol. Cell *30*, 393–402.

Kaelin, W.G., Jr., and Thompson, C.B. (2010). Q&A: Cancer: clues from cell metabolism. Nature *465*, 562–564.

King, A., Selak, M.A., and Gottlieb, E. (2006). Succinate dehydrogenase and fumarate hydratase: linking mitochondrial dysfunction and cancer. Oncogene *25*, 4675–4682.

Kondo, K., Klco, J., Nakamura, E., Lechpammer, M., and Kaelin, W.G., Jr. (2002). Inhibition of HIF is necessary for tumor suppression by the von Hippel-Lindau protein. Cancer Cell *1*, 237–246.

Laderoute, K.R., Amin, K., Calaoagan, J.M., Knapp, M., Le, T., Orduna, J., Foretz, M., and Viollet, B. (2006). 5′-AMP-activated protein kinase (AMPK) is induced by low-oxygen and glucose deprivation conditions found in solid-tumor microenvironments. Mol. Cell. Biol. *26*, 5336–5347.

Launonen, V., Vierimaa, O., Kiuru, M., Isola, J., Roth, S., Pukkala, E., Sistonen, P., Herva, R., and Aaltonen, L.A. (2001). Inherited susceptibility to uterine leiomyomas and renal cell cancer. Proc. Natl. Acad. Sci. USA *98*, 3387–3392.

LaVaute, T., Smith, S., Cooperman, S., Iwai, K., Land, W., Meyron-Holtz, E., Drake, S.K., Miller, G., Abu-Asab, M., Tsokos, M., et al. (2001). Targeted deletion of the gene encoding iron regulatory protein-2 causes misregulation of iron metabolism and neurodegenerative disease in mice. Nat. Genet. *27*, 209–214.

Luo, Z., Saha, A.K., Xiang, X., and Ruderman, N.B. (2005). AMPK, the metabolic syndrome and cancer. Trends Pharmacol. Sci. *26*, 69–76.

Maffettone, C., Chen, G., Drozdov, I., Ouzounis, C., and Pantopoulos, K. (2010). Tumorigenic properties of iron regulatory protein 2 (IRP2) mediated by its specific 73-amino acids insert. PLoS ONE *5*, e10163.

Maranchie, J.K., Vasselli, J.R., Riss, J., Bonifacino, J.S., Linehan, W.M., and Klausner, R.D. (2002). The contribution of VHL substrate binding and HIF1-alpha to the phenotype of VHL loss in renal cell carcinoma. Cancer Cell *1*, 247–255.

Marsin, A.S., Bertrand, L., Rider, M.H., Deprez, J., Beauloye, C., Vincent, M.F., Van den Berghe, G., Carling, D., and Hue, L. (2000). Phosphorylation and activation of heart PFK-2 by AMPK has a role in the stimulation of glycolysis during ischaemia. Curr. Biol. *10*, 1247–1255.

Menendez, J.A., and Lupu, R. (2007). Fatty acid synthase and the lipogenic phenotype in cancer pathogenesis. Nat. Rev. Cancer *7*, 763–777.

Merino, M.J., Torres-Cabala, C., Pinto, P., and Linehan, W.M. (2007). The morphologic spectrum of kidney tumors in hereditary leiomyomatosis and renal cell carcinoma (HLRCC) syndrome. Am. J. Surg. Pathol. *31*, 1578–1585.

Mims, M.P., and Prchal, J.T. (2005). Divalent metal transporter 1. Hematology *10*, 339–345.

Muckenthaler, M.U., Galy, B., and Hentze, M.W. (2008). Systemic iron homeostasis and the iron-responsive element/iron-regulatory protein (IRE/IRP) regulatory network. Annu. Rev. Nutr. *28*, 197–213.

Musi, N., Hayashi, T., Fujii, N., Hirshman, M.F., Witters, L.A., and Goodyear, L.J. (2001). AMP-activated protein kinase activity and glucose uptake in rat skeletal muscle. Am. J. Physiol. Endocrinol. Metab. *280*, E677–E684.

Pollard, P.J., Brière, J.J., Alam, N.A., Barwell, J., Barclay, E., Wortham, N.C., Hunt, T., Mitchell, M., Olpin, S., Moat, S.J., et al. (2005). Accumulation of Krebs cycle intermediates and over-expression of HIF1alpha in tumours which result from germline FH and SDH mutations. Hum. Mol. Genet. *14*, 2231–2239.

Pollard, P.J., Spencer-Dene, B., Shukla, D., Howarth, K., Nye, E., El-Bahrawy, M., Deheragoda, M., Joannou, M., McDonald, S., Martin, A., et al. (2007). Targeted inactivation of fh1 causes proliferative renal cyst development and activation of the hypoxia pathway. Cancer Cell *11*, 311–319.

Puig, S., Vergara, S.V., and Thiele, D.J. (2008). Cooperation of two mRNA-binding proteins drives metabolic adaptation to iron deficiency. Cell Metab. *7*, 555–564.

Raval, R.R., Lau, K.W., Tran, M.G., Sowter, H.M., Mandriota, S.J., Li, J.L., Pugh, C.W., Maxwell, P.H., Harris, A.L., and Ratcliffe, P.J. (2005). Contrasting properties of hypoxia-inducible factor 1 (HIF-1) and HIF-2 in von Hippel-Lindau-associated renal cell carcinoma. Mol. Cell. Biol. *25*, 5675–5686.

Rouault, T.A. (2006). The role of iron regulatory proteins in mammalian iron homeostasis and disease. Nat. Chem. Biol. *2*, 406–414.

Sanchez, M., Galy, B., Muckenthaler, M.U., and Hentze, M.W. (2007). Iron-regulatory proteins limit hypoxia-inducible factor-2alpha expression in iron deficiency. Nat. Struct. Mol. Biol. *14*, 420–426.

Semenza, G.L. (2009). Regulation of cancer cell metabolism by hypoxia-inducible factor 1. Semin. Cancer Biol. *19*, 12–16.

Shaw, R.J. (2006). Glucose metabolism and cancer. Curr. Opin. Cell Biol. *18*, 598–608.

Sudarshan, S., Sourbier, C., Kong, H.S., Block, K., Valera Romero, V.A., Yang, Y., Galindo, C., Mollapour, M., Scroggins, B., Goode, N., et al. (2009). Fumarate hydratase deficiency in renal cancer induces glycolytic addiction and hypoxia-inducible transcription factor 1alpha stabilization by glucose-dependent generation of reactive oxygen species. Mol. Cell. Biol. *29*, 4080–4090.

Sun, F., Huo, X., Zhai, Y., Wang, A., Xu, J., Su, D., Bartlam, M., and Rao, Z. (2005). Crystal structure of mitochondrial respiratory membrane protein complex II. Cell *121*, 1043–1057.

Tabuchi, M., Tanaka, N., Nishida-Kitayama, J., Ohno, H., and Kishi, F. (2002). Alternative splicing regulates the subcellular localization of divalent metal transporter 1 isoforms. Mol. Biol. Cell *13*, 4371–4387.

Tomlinson, I.P., Alam, N.A., Rowan, A.J., Barclay, E., Jaeger, E.E., Kelsell, D., Leigh, I., Gorman, P., Lamlum, H., Rahman, S., et al; Multiple Leiomyoma Consortium. (2002). Germline mutations in FH predispose to dominantly inherited uterine fibroids, skin leiomyomata and papillary renal cell cancer. Nat. Genet. *30*, 406–410.

Toro, J.R., Nickerson, M.L., Wei, M.H., Warren, M.B., Glenn, G.M., Turner, M.L., Stewart, L., Duray, P., Tourre, O., Sharma, N., et al. (2003). Mutations in the fumarate hydratase gene cause hereditary leiomyomatosis and renal cell cancer in families in North America. Am. J. Hum. Genet. *73*, 95–106.

Tsuji, Y., Akebi, N., Lam, T.K., Nakabeppu, Y., Torti, S.V., and Torti, F.M. (1995). FER-1, an enhancer of the ferritin H gene and a target of E1A-mediated transcriptional repression. Mol. Cell. Biol. *15*, 5152–5164.

Vander Heiden, M.G., Cantley, L.C., and Thompson, C.B. (2009). Understanding the Warburg effect: the metabolic requirements of cell proliferation. Science *324*, 1029–1033.

Vousden, K.H., and Ryan, K.M. (2009). p53 and metabolism. Nat. Rev. Cancer *9*, 691–700.

Warburg, O. (1956). On the origin of cancer cells. Science *123*, 309–314.

Wu, K.J., Polack, A., and Dalla-Favera, R. (1999). Coordinated regulation of iron-controlling genes, H-ferritin and IRP2, by c-MYC. Science *283*, 676–679.

Xiang, X., Saha, A.K., Wen, R., Ruderman, N.B., and Luo, Z. (2004). AMP-activated protein kinase activators can inhibit the growth of prostate cancer cells by multiple mechanisms. Biochem. Biophys. Res. Commun. *321*, 161–167.

Yang, Y., Valera, V.A., Padilla-Nash, H.M., Sourbier, C., Vocke, C.D., Vira, M.A., Abu-Asab, M.S., Bratslavsky, G., Tsokos, M., Merino, M.J., et al. (2010). UOK 262 cell line, fumarate hydratase deficient (FH-/FH-) hereditary leiomyomatosis renal cell carcinoma: in vitro and in vivo model of an aberrant energy metabolic pathway in human cancer. Cancer Genet. Cytogenet. *196*, 45–55.

Zhang, F., Wang, W., Tsuji, Y., Torti, S.V., and Torti, F.M. (2008). Post-transcriptional modulation of iron homeostasis during p53-dependent growth arrest. J. Biol. Chem. *283*, 33911–33918.

Zhang, H., Cicchetti, G., Onda, H., Koon, H.B., Asrican, K., Bajraszewski, N., Vazquez, F., Carpenter, C.L., and Kwiatkowski, D.J. (2003). Loss of Tsc1/Tsc2 activates mTOR and disrupts PI3K-Akt signaling through downregulation of PDGFR. J. Clin. Invest. *112*, 1223–1233.

Zimmer, M., Ebert, B.L., Neil, C., Brenner, K., Papaioannou, I., Melas, A., Tolliday, N., Lamb, J., Pantopoulos, K., Golub, T., and Iliopoulos, O. (2008). Small-molecule inhibitors of HIF-2a translation link its 5′UTR iron-responsive element to oxygen sensing. Mol. Cell *32*, 838–848.